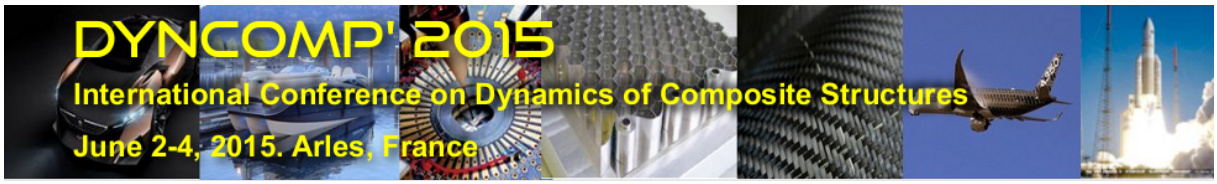

ENERGY FLOW PREDICTION IN PIEZOELECTRIC COMPOSITE STRUCTURES THROUGH A HYBRID FINITE ELEMENT/WAVE AND FINITE ELEMENT APPROACH

Y. Fan[1], M. Collet[1], M. Ichchou[1*], O. Bareille[1] and Z. Dimitrijevic[2]

[1]Laboratoire de Tribologie et Dynamique des Systèmes (LTDS)
Ecole Centrale de Lyon, 69134 Ecully Cedex, FRANCE
Email: mohamed.ichchou@ec-lyon.fr, yu.fan@ec-lyon.fr

[2]PSA Peugeot-Citroën
F-78943 Vélizy Villacoublay Cedex, FRANCE
Email: zoran.dimitrijevic@mpsa.com

ABSTRACT

The vibration and noise of a structure can be mitigated by controlling the power exchange between the excitation and the remote parts. An implementation is to integrate piezoelectric materials into the host structure and to design the associated electric impedance in order to control the energy flow. In this work, built-up structures with periodical piezoelectric shunts are considered. Major efforts are devoted to develop a rapid and accurate numerical tool for the evaluation of the energy flow in this kind of built-up structures. In this method, Wave and Finite Element Method (WFEM) is employed to model the periodic substructures while Finite Element Method (FEM) is used to capture the non-periodic substructures. A modal reduction technique is introduced to WFEM accelerate the wave basis calculation. Validations are presented, attesting the accuracy of he proposed method. An application is given, where energy flow of a infinite structure with resistive piezoelectric waveguide is presented.

1 INTRODUCTION

To control the energy transmission through the excitation to the remote parts, one method is to periodically distribute piezoelectric patches with identical circuits between the source (termed *near-field* substructure) and the remote parts (termed *far-field* substructure), shown in figure 1. This idea was considered in [1] and [2] to reduce the vibration in rotational components in aero-engine. It has been shown that periodically distributed piezoelectric shunts can control the localized vibration in near-periodic structures [2] and also can reduce the response to the engine order excitation in periodic structures [1]. Alternatively, the wave perspective was considered in [3, 4], where the functions of piezoelectric patches are to reflect the injected waves or to welcome the waves and dissipate them. To evaluate the performance of the piezoelectric waveguide as a component in a built-up structure, a numerical tool for the forced response and energy flow in these built-up structures are required.

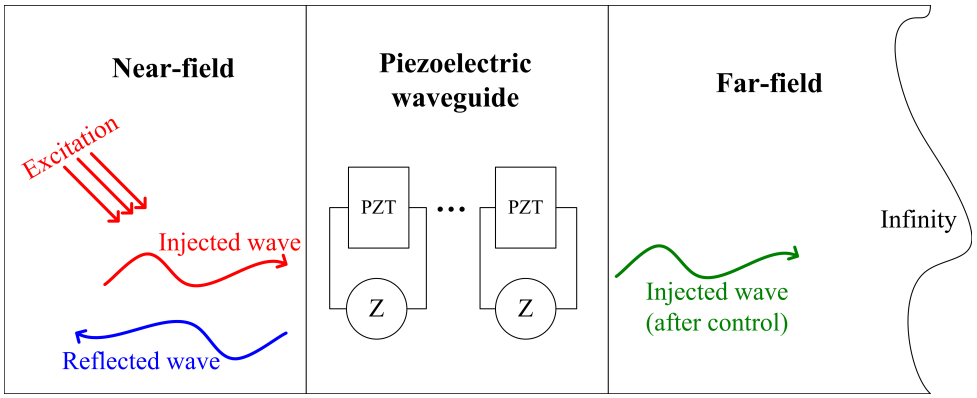

Figure 1: Illustration of the considered piezoelectric-based built-up structures

In this work, a hybrid finite element method (FEM) /wave and finite element method (WFEM) is developed to determine the forced response and energy flow of built-up structure with periodic piezoelectric patches. The near-field is supposed to be non-periodic so it is modeled by FEM. The piezoelectric substructure and the far-field are regarded as waveguide and they are modeled by WFEM. By WFEM, the dynamics of the periodic waveguide would be analyzed by only considering one segment of it, hence the computation time is saved. The engineering example is shown in figure 2 where a car chassis is considered. The domain near the engine can be regarded as near-field while the car body connected to the frame can be treated as far-field. Piezoelectric patches can be periodically bonded to the frame so that it can be treated as a periodic waveguide.

Specifically, a modal reduction approach is introduced into the WFEM to accelerate the wave basis calculation. It is useful especially when the DOFs of the cross-session are numerous. Moreover, only the DOFs of the FE modeled near-field will be kept while the ones of the waveguides will be eliminated eventually. Then the response and energy flow can be obtained by post-processing in a multi-scale manner. The far-field substructure can be both finite and infinite, so this method is applicable in both mode-dominated (low frequency) cases [5] and the wave-dominated (mid- and high frequencies) cases [6].

In the following sections, firstly the enhanced WFEM is briefly introduced. Then the way to adapt the WFEM modeled waveguides into the FEM modeled near-field is presented. A validation is presented where finite far-field substructures are considered and each piezoelectric

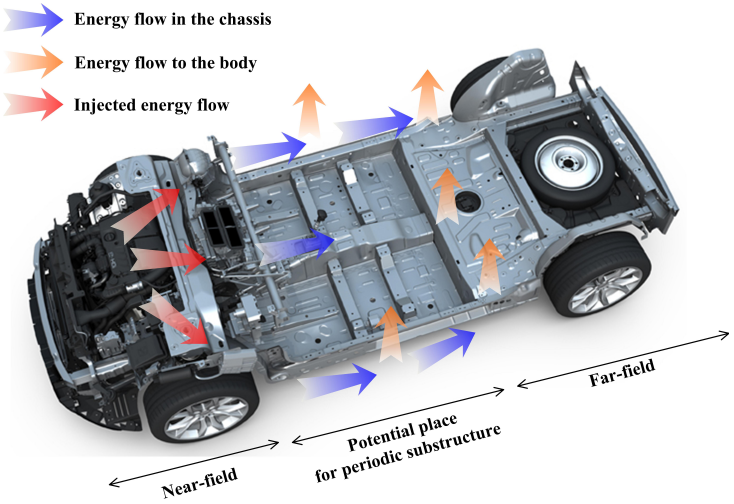

Figure 2: An engineering example of the considered structures

patch is shunted by an identical Resistor-inductor circuit. At the end an application is presented where the energy flow to a infinite far-field is presented.

2 ENHANCED WAVE AND FINITE ELEMENT METHOD

2.1 Modal condensation of a unit cell

In WFEM, the dynamics of the whole periodic waveguide can be described only by analyzing one unit cell of the waveguide thanks to Bloch theorem. The dynamics equations of a unit cell in the periodic waveguide can be formed by any existed FEM package and they write

$$\begin{bmatrix} \mathbf{H}_{ii} & \mathbf{H}_{ib} \\ \mathbf{H}_{bi} & \mathbf{H}_{bb} \end{bmatrix} \begin{pmatrix} \mathbf{q}_i \\ \mathbf{q}_b \end{pmatrix} = \begin{pmatrix} \mathbf{0} \\ \mathbf{f}_b \end{pmatrix} \tag{1}$$

where superscripts i and b respectively refer to the internal and the boundary DOFs. Splitting boundary DOFs on left (subscript L) and right (subscript R) interfaces, it gives $\mathbf{q}_b = \begin{pmatrix} \mathbf{q}_L^T & \mathbf{q}_R^T \end{pmatrix}^T$ and $\mathbf{f}_b = \begin{pmatrix} \mathbf{f}_L^T & \mathbf{f}_R^T \end{pmatrix}^T$. The terms are illustrated in figure 3. Then the internal DOFs would be condensed so that equation (1) becomes

$$\mathbf{D}\mathbf{q}_b = \mathbf{f}_b \tag{2}$$

where

$$\mathbf{D} = \mathbf{H}_{bb} - \mathbf{H}_{bi}\mathbf{H}_{ii}^{-1}\mathbf{H}_{ib} \tag{3}$$

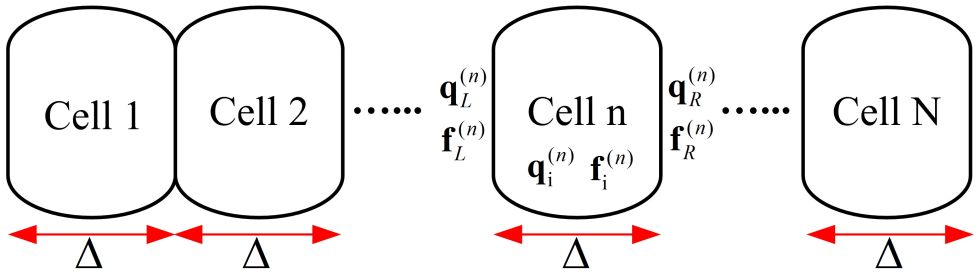

Figure 3: Illustration of the unit cells in a waveguide

Searching for the inverse of $\mathbf{H}_{ii}$ might be time consuming once the number of the internal DOFs is large. Alternatively, it is better to firstly reduce the dimension of the matrices before the condensation as proposed by [7]. In their work, the Craig Bampton method for modal reduction was employed on all the internal DOFs. Here the major concern is that not all the DOFs in $\mathbf{q}_i$ is suitable to be transferred to modal space and be reduced. The DOFs associated with the electric field are better not to be transferred into the modal space. There are two reasons. Firstly the impedance of the electric circuits need to be changed in the calculations so as to evaluate the performance under different parameters. If they are transferred to the modal space it would be difficult to change the corresponding modal impedance for each retained modes [3]. Otherwise the modal transformation need to be performed once again, after each electric impedance modification. Secondly, if electric impedance are considered in the shunted circuits, the dynamic stiffness matrix can no longer be diagonalized by the open-circuit or close-circuit modal shapes. Consequently the modal coordinates might be coupled with each other due to non-diagonal damping terms, then simply remove the modes with higher natural frequencies might induce unexpected errors.

For these reasons, we rewrite array $\mathbf{q}_i$ into $\begin{pmatrix} \mathbf{q}_c^T & \mathbf{q}_n^T \end{pmatrix}^T$ where $\mathbf{q}_c$ represents all the mechanical DOFs and $\mathbf{q}_n$ for the electric ones. Then only the DOFs in $\mathbf{q}_c$ are transferred into the modal coordinates $\mathbf{y}$ by

$$\begin{pmatrix} \mathbf{q}_i \\ \mathbf{q}_b \end{pmatrix} = \begin{pmatrix} \mathbf{q}_c \\ \mathbf{q}_n \\ \mathbf{q}_b \end{pmatrix} = \begin{bmatrix} \Psi & -\mathbf{K}_{cc}^{-1}\mathbf{K}_{cn} & -\mathbf{K}_{cc}^{-1}\mathbf{K}_{cb} \\ \mathbf{0} & \mathbf{I} & \mathbf{0} \\ \mathbf{0} & \mathbf{0} & \mathbf{I} \end{bmatrix} \begin{pmatrix} \mathbf{y} \\ \mathbf{q}_n \\ \mathbf{q}_b \end{pmatrix} \tag{4}$$

where $\Psi = \begin{bmatrix} \psi_1 & \psi_2 & \cdots & \psi_l \end{bmatrix}$. ψ_k is the kth natural mode of the unit cell with all rest DOFs fixed ($\mathbf{q}_b = \mathbf{0}$ and $\mathbf{q}_n = \mathbf{0}$) and the corresponding natural frequencies is ω_k. Specifically, ψ_k and ω_k with $k = 1, 2, \cdots, l$ are obtained as the eigenvectors and eigenvalues of

$$\left(\mathbf{K}_{cc} - \omega_i^2 \mathbf{M}_{cc}\right) \psi_i = \mathbf{0} \tag{5}$$

Only l modes are kept in Ψ, and the number is less than that of $\mathbf{q}_c$. The criterion for the selection of the retained modes is $\omega_k < 3\omega_m$ where ω_m is the maximum excitation frequency to be considered. Introduce the transformation (4) into equation (1), the dynamical equations can be reduced to

$$\begin{bmatrix} \hat{\mathbf{H}}_{cc} & \hat{\mathbf{H}}_{cn} & \hat{\mathbf{H}}_{cb} \\ \hat{\mathbf{H}}_{nc} & \hat{\mathbf{H}}_{nn} & \hat{\mathbf{H}}_{nb} \\ \hat{\mathbf{H}}_{bc} & \hat{\mathbf{H}}_{bn} & \hat{\mathbf{H}}_{bb} \end{bmatrix} \begin{pmatrix} \mathbf{y} \\ \mathbf{q}_n \\ \mathbf{q}_b \end{pmatrix} = \begin{pmatrix} \mathbf{f}_y \\ \mathbf{f}_n \\ \mathbf{f}_b \end{pmatrix} \tag{6}$$

where

$$\hat{\mathbf{H}}_{cc} = \begin{bmatrix} \ddots & & \\ & 1 - \omega_k^2 + 2j\xi_k\omega_k & \\ & & \ddots \end{bmatrix} \tag{7}$$

Then the electromechanical coupling is already integrated into matrix $\mathbf{H}$ in the FEM procedure. While the electric impedance matrix $\mathbf{Z}$ can be introduced by adding relation $\mathbf{f}_n = -\mathbf{Z}\mathbf{q}_n$ in equation (6). Eliminating $\mathbf{y}$ and $\mathbf{q}_n$ in equation (6) when no external forces are applied to the internal DOFs ($\mathbf{f}_y = \mathbf{0}$ and $\mathbf{f}_n = \mathbf{0}$), we can also obtain the same form as shown in equation (2) by

$$\mathbf{D} = \hat{\mathbf{H}}_{bb} - \hat{\mathbf{H}}_{bi}\hat{\mathbf{H}}_{ii}^{-1}\hat{\mathbf{H}}_{ib} \tag{8}$$

where

$$\hat{\mathbf{H}}_{ii} = \begin{bmatrix} \hat{\mathbf{H}}_{cc} & \hat{\mathbf{H}}_{cn} \\ \hat{\mathbf{H}}_{nc} & \hat{\mathbf{H}}_{nn} + \mathbf{Z} \end{bmatrix} \tag{9}$$

Less computational cost are required because $\hat{\mathbf{H}}_{\mathrm{ii}}$ is a sparse matrix with a much smaller size in comparison with $\mathbf{H}_{\mathrm{ii}}$.

2.2 Wave basis: a selected set of characteristic waves

According to Bloch theory, the free wave of the form $e^{j\omega t-kx}$ that travels in the periodic structure should satisfy the condition

$$\mathbf{q}_{\mathrm{R}}^{(n)} = \lambda \mathbf{q}_{\mathrm{L}}^{(n)} \tag{10}$$

while the equilibrium implies that

$$\mathbf{f}_{\mathrm{R}}^{(n)} = -\lambda \mathbf{f}_{\mathrm{L}}^{(n)} \tag{11}$$

where $\lambda = e^{-jk\Delta}$ describes the amplitude and phase change when the wave propagates from the left side to the right side of a unit cell. k is the wavenumber and Δ is the length of a unit cell. Introduce equation (10) and (11) into (2) and eliminate $\mathbf{f}_{\mathrm{L}}$ and $\mathbf{f}_{\mathrm{R}}$, leads to

$$\left(\begin{bmatrix} \mathbf{0} & \sigma\mathbf{I} \\ -\mathbf{D}_{\mathrm{RL}} & -\mathbf{D}_{\mathrm{RR}} \end{bmatrix} - \begin{bmatrix} \sigma\mathbf{I} & \mathbf{0} \\ \mathbf{D}_{\mathrm{LL}} & \mathbf{D}_{\mathrm{LR}} \end{bmatrix} \right) \begin{pmatrix} \mathbf{q}_{\mathrm{L}} \\ \mathbf{q}_{\mathrm{R}} \end{pmatrix} = \mathbf{0} \tag{12}$$

Assembling the displacement and force eigenvectors in the matrix form we obtain the wave basis

$$\Phi = \begin{bmatrix} \Phi_{\mathrm{q}}^{+} & \Phi_{\mathrm{q}}^{-} \\ \Phi_{\mathrm{f}}^{+} & \Phi_{\mathrm{f}}^{-} \end{bmatrix} \tag{13}$$

where superscript $+$ and $-$ refer to the data belong to positive and negative going waves respectively. It is not necessary to consider all the N waves, because those strong evanescent waves nearly have no contribution to the overall response while they cause numerical issues [8, 9]. The m kept waves are those propagating ($|\lambda| = 1$) and less decaying ($|\lambda| > \tau$), where τ is a given factor, here is $\tau = 0.01$ is used. Because of the wave selection, the number of waves to be kept can be different in different frequencies.

3 DYNAMIC STIFFNESS MATRIX OF THE BUILT-UP STRUCTURE

Concerning the analysis of the complete assembled structure, there are 3 major steps, as shown in figure 4: 1) model the near-field completely by FEM, with no reduction or simplification; 2) model the far-field waveguide by WFEM and obtained the equivalent reflection matrix; and 3) model the piezoelectric waveguide and obtain the equivalent mechanical impedance matrix.

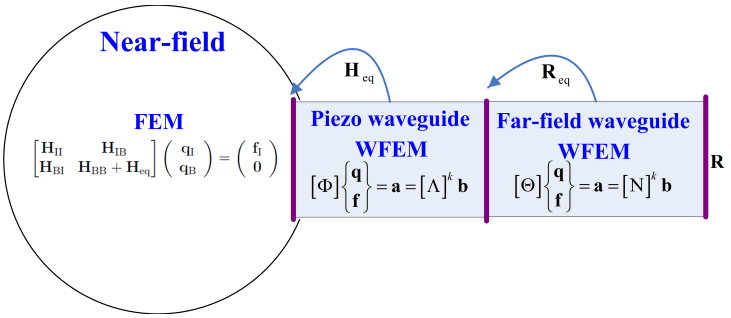

Figure 4: Illustration of the modeling process of the proposed method.

After these steps, all the DOFs of the waveguides would be condensed so that the final dimension of the dynamics stiffness matrix of the built-up structure is equal to the near field

one. The governing equations then write

$$\begin{bmatrix} \mathbf{H}_{\mathrm{II}} & \mathbf{H}_{\mathrm{IB}} \\ \mathbf{H}_{\mathrm{BI}} & \mathbf{H}_{\mathrm{BB}} + \mathbf{H}_{\mathrm{eq}} \end{bmatrix} \begin{pmatrix} \mathbf{q}_{\mathrm{I}} \\ \mathbf{q}_{\mathrm{B}} \end{pmatrix} = \begin{pmatrix} \mathbf{f}_{\mathrm{I}} \\ \mathbf{0} \end{pmatrix} \tag{14}$$

where subscripts $\mathbf{I}$ and $\mathbf{B}$ indicate the internal DOFs of the near-field and the DOFs connected to the waveguides respectively. $\mathbf{H}_{\mathrm{eq}}$ is the equivalent mechanical impedance of piezoelectric waveguide and it is

$$\mathbf{H}_{\mathrm{eq}} = \left[\Phi_{\mathrm{f}}^{+} + \Phi_{\mathrm{f}}^{-}\left({}^{-}\Lambda^{-L_{\mathrm{p}}/\Delta_{p}} \cdot \mathbf{R}_{\mathrm{eq}} \cdot {}^{+}\Lambda^{L_{\mathrm{p}}/\Delta_{\mathrm{p}}}\right)\right]\left[\Phi_{\mathrm{q}}^{+} + \Phi_{\mathrm{q}}^{-}\left({}^{-}\Lambda^{-L_{\mathrm{p}}/\Delta_{\mathrm{p}}} \cdot \mathbf{R}_{\mathrm{eq}} \cdot {}^{+}\Lambda^{L_{\mathrm{p}}/\Delta_{\mathrm{p}}}\right)\right]^{-1} \tag{15}$$

where $\mathbf{R}_{eq}$ is the equivalent reflection matrix of the far-field substructure. Specifically, it is

$$\mathbf{R}_{\mathrm{eq}} = -\left(\Phi_{\mathrm{q}}^{-} - \mathbf{Y}\Phi_{\mathrm{f}}^{-}\right)^{-1}\left(\Phi_{\mathrm{q}}^{+} - \mathbf{Y}\Phi_{\mathrm{f}}^{+}\right) \tag{16}$$

and

$$\mathbf{Y} = \left[\Theta_{\mathrm{q}}^{+} + \Theta_{\mathrm{q}}^{-}\left({}^{-}\mathbf{N}^{-L_{\mathrm{f}}/\Delta_{\mathrm{f}}} \cdot \mathbf{R} \cdot {}^{+}\mathbf{N}^{L_{\mathrm{f}}/\Delta_{\mathrm{f}}}\right)\right]\left[\Theta_{\mathrm{f}}^{+} + \Theta_{\mathrm{f}}^{-}\left({}^{-}\mathbf{N}^{-L_{\mathrm{f}}/\Delta_{\mathrm{f}}} \cdot \mathbf{R} \cdot {}^{+}\mathbf{N}^{L_{\mathrm{f}}/\Delta_{\mathrm{f}}}\right)\right]^{-1} \tag{17}$$

where $\mathbf{R}$ is the reflection matrix at the boundary of far-field substructure. For infinite case it is a zero matrix. ${}^{+}\Lambda$ and ${}^{-}\Lambda$ are diagonal matrices consisted of wavenumbers associated to positive-going and negative-going waves in piezoelectric waveguide respectively. ${}^{+}\mathbf{N}$ and ${}^{-}\mathbf{N}$ have the same meaning but they are for far-field waveguide. Φ and Θ represent the wave basis for piezoelectric waveguide and far-field waveguide respectively.

4 VALIDATIONS

A finite solid-element meshed structure is considered, shown in figure 5. It is constructed by bonding 10 groups of co-located piezoelectric patches onto a uniform host structure excited at the center. 5 groups of piezoelectric patches are periodically distributed at the right side of the excitation while five other groups are located on the other side. The structure is clamped on the right top and free at the left end.

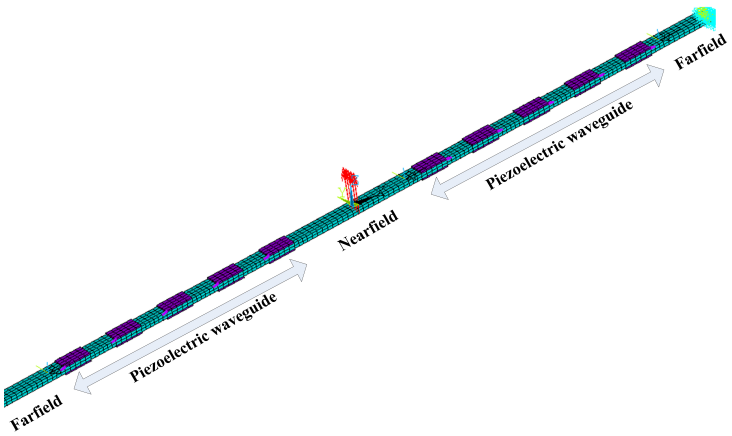

Figure 5: The calculation layout of the finites piezoelectric structure

To establish the wave basis of the piezoelectric waveguides, the proposed modal reduction approach is employed. All the internal mechanical DOFs have been transferred into modal coordinates and only 10 modal DOFs are retained. While all the electric DOFs remain in the

reduced dynamic stiffness matrix. Figure 6 compares the stiffness matrix of a unit cell before and after the modal reduction in the form $log_{10}(|\cdot|)$. It can be seen in figure 6a that, before the reduction, the matrix is sparse and large (722×722). While after the reduction it tends to be dense and with a much smaller size (102×102). In the condensation process, 90 boundary DOFs are retained, which means only a 12×12 matrix of the internal DOFs needs to be inverted after the reduction, otherwise the inverse of a 632×632 matrix of the internal DOFs will be searched.

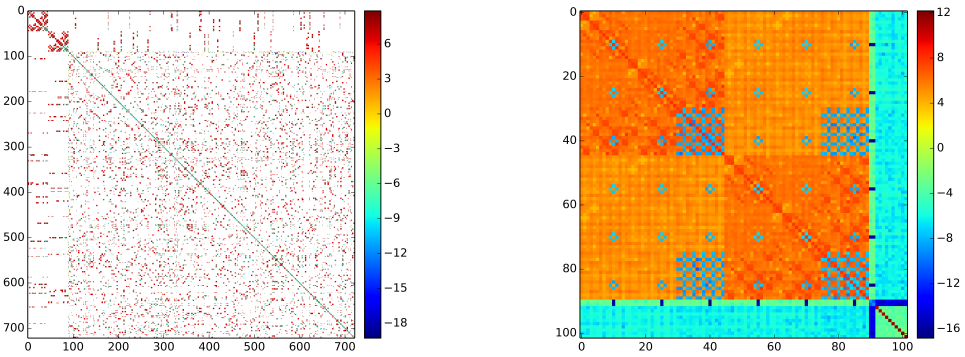

(a) Before modal reduction (b) After modal reduction

Figure 6: Illustration of stiffness matrix of a unit cell

The dispersion curves of the piezoelectric waveguides are shown in figure 7a. Overall 6 waves are observed after the identification, in which 4 waves (wave index 0, 1, 4 and 5) are propagating and 2 waves (wave index 2 and 3) are evanescent. Their wave shapes indicate that wave 0 and 2 are propagating (figure 7b) and evanescent flexural waves in z direction respectively , wave 1 and 3 are the propagating and evanescent flexural waves in y direction, wave 4 is the torsional wave and wave 5 is the longitudinal wave.

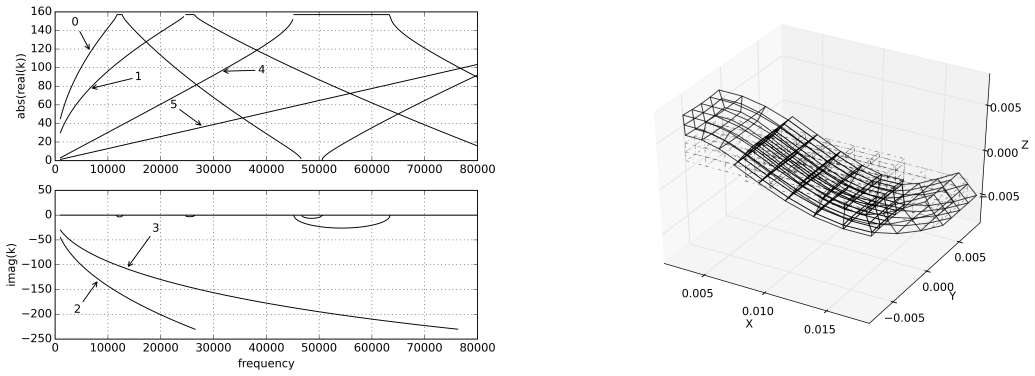

(a) The dispersion curves (b) wave shape 0: flexural

Figure 7: Wave modal results of the piezoelectric waveguide

With the reduced wave bases of the piezoelectric and far-field waveguides, the proposed method can be employed to analyze the forced response of the structure. The validation data come from the full FE model of the whole assembled structure. Two circuits are considered: 1)

resistor $R = 1 \times 10^5\,\Omega$; and 2) resistor-inductor $R = 10\,\Omega$ and $L = 2.945\,\mathrm{H}$. The response is compared between full FE model and the proposed hybrid model, shown in figure 8. The results of the proposed method are first obtained only on the near-field DOFs. Then the response of the waveguides are obtained progressively by post-processing. Good agreements can be seen in both figures. It should be noted that two reduction have been made on different stages. To obtain the wave basis, a structural-modal reduction was conducted in order to accelerate the calculation. Additionally, in forced response analysis, a wave-modal reduction was employed to avoid ill-conditioning. In this validation case, 10 of the overall 632 structural modes are retained in the first reduction and concerning the later reduction only 6 of the overall 45 waves in the piezoelectric waveguides and 42 waves of the overall 45 waves in far-field waveguides are kept. The agreement with the full model results indicate that these reductions are accurate and the proposed method is applicable to solid-element modeling case.

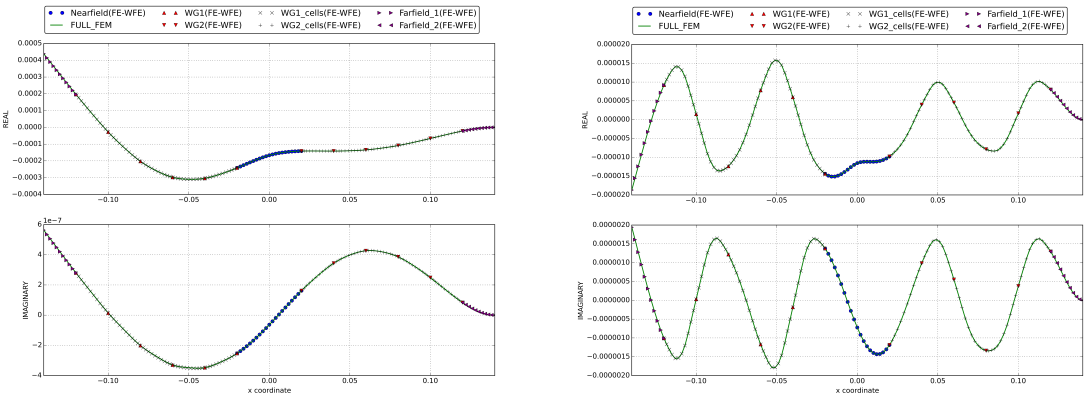

(a) With resistive circuit at 400 Hz

(b) With resistor-inductor circuit at 3120 Hz

Figure 8: Validation of the proposed method with full FEM results: displacement of u_z DOF of all the middle line nodes

5 APPLICATION

The proposed numerical tool also enables one to analyze the energy flow and forced response in open structural system constructed by a near-field and several periodic waveguides. Here an application is briefly presented. The considered open structural system is obtained by changing the far-field of the closed structural system used in the validation to infinite. The material properties, the geometric of near-field and the parameters of a single unit cell of the waveguides remain the same. Each piezoelectric patch is shunted by an identical resistive circuit, where resistance $R = 1 \times 10^4\,\Omega$. The excitation is applied in the center of the near-field, still as same as it was considered in the validation.

Forced response and energy flow are obtained by the proposed method and presented in figure 9, where only the data in positive x coordinates are presented due to the symmetry of the structure. The contribution to the displacement of the evanescent waves can be seen in the near-field. In the Far-field, propagating waves dominate the response where the phase varies linearly in space. Through the results of energy flow, the dissipation caused by the piezoelectric waveguide are clearly illustrated.

To find the desired design of the piezoelectric waveguide, one needs to choose a patten of

the electric circuit and calculate the power flow with different parameters. Sometimes maybe a optimization process will be connected. Due to the dual condensation condensations considered in this method, it is suitable for this kind of repetitive calculation.

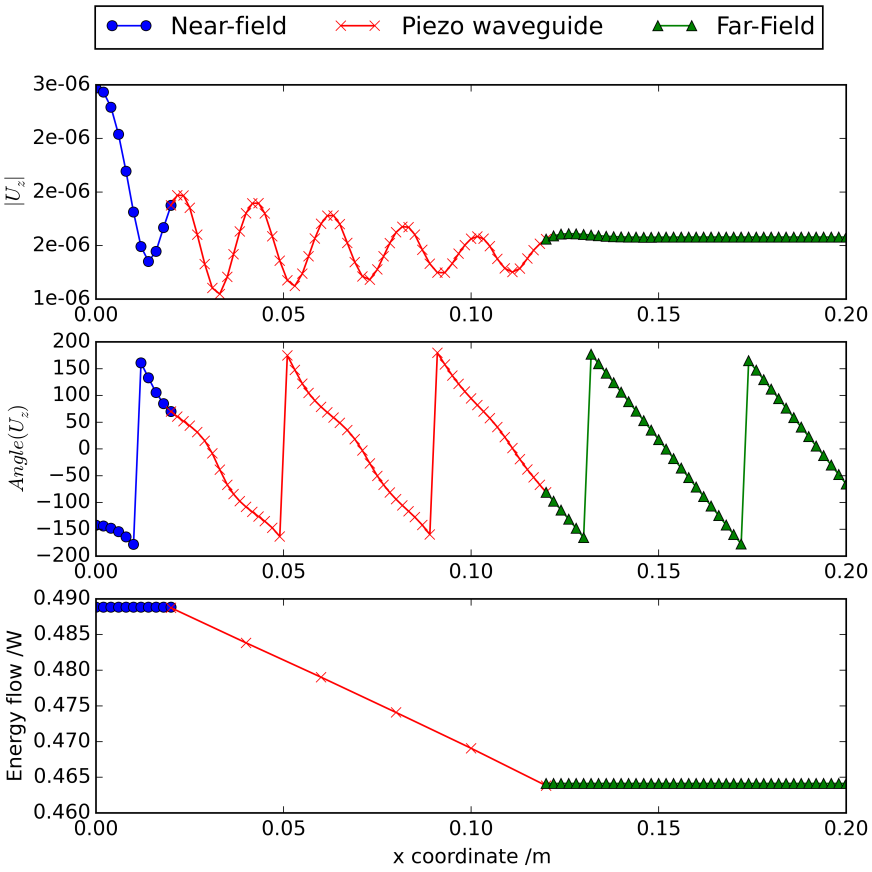

Figure 9: Forced response and energy flow in the structure

6 CONCLUDING REMARKS

A multi-scale numerical tool for the forced response and energy flow for piezoelectric-based structures are proposed in this paper. By means of this approach, the designed 1D piezoelectric waveguides can be evaluated by considering them as components of a built-up structure. The major modeling strategy is to model the non-periodic near-field by FEM and the waveguides by an enhanced WFEM, and then adapt the models of the substructures. The correlation with full FEM results attests that the proposed method is also accurate to simulate mode-dominated finite structures. With the advantage in the calculation speed, this method is applicable in the design process where the calculation is required on numerous sets of parameters.

REFERENCES

[1] Yu Fan and Lin Li. Vibration Dissipation Characteristics of Symmetrical Piezoelectric Networks With Passive Branches. In *ASME Turbo Expo 2012: Turbine Technical Conference and Exposition, Volume 7: Structures and Dynamics, Parts A and B*, pages 1263–1273. ASME, June 2012.

[2] Hongbiao Yu and K. W. Wang. Vibration Suppression of Mistuned Coupled-Blade-Disk Systems Using Piezoelectric Circuitry Network. *Journal of Vibration and Acoustics*, 131(2):021008, 2009.

[3] M. Collet, K.a. Cunefare, and M.N. Ichchou. Wave Motion Optimization in Periodically Distributed Shunted Piezocomposite Beam Structures. *Journal of Intelligent Material Systems and Structures*, 20(7):787–808, October 2008.

[4] O Thorp, M Ruzzene, and a Baz. Attenuation and localization of wave propagation in rods with periodic shunted piezoelectric patches. *Smart Materials and Structures*, 10(5):979–989, 2001.

[5] Lin Li and Peiyi Wang. Evaluation of High-Order Resonance of Blade Under Wake Excitation. In *ASME Turbo Expo 2010: Power for Land, Sea, and Air, Volume 6: Structures and Dynamics, Parts A and B*, pages 995–1001. ASME, October 2010.

[6] H.G.D. Goyder and R.G. White. Vibrational power flow from machines into built-up structures, part III: Power flow through isolation systems. *Journal of Sound and Vibration*, 68(1):97–117, January 1980.

[7] Changwei Zhou. *Wave and modal coupled approach for multi-scale analysis of periodic structures*. Phd thesis, Ecole Centrale de Lyon, 2014.

[8] Y. Waki, B.R. Mace, and M.J. Brennan. Free and forced vibrations of a tyre using a wave/finite element approach. *Journal of Sound and Vibration*, 323(3-5):737–756, June 2009.

[9] W.J. Zhou and M.N. Ichchou. Wave propagation in mechanical waveguide with curved members using wave finite element solution. *Computer Methods in Applied Mechanics and Engineering*, 199(33-36):2099–2109, July 2010.

COPYRIGHT NOTICE

Copyright ©2015 by the authors. Distribution of all material contained in this paper is permitted under the terms of the Creative Commons license Attribution-NonCommercial-NoDerivatives 4.0 International (CC-by-nc-nd 4.0).